

# Quaternary structure of alpha-crustacyanin from lobster as seen by small-angle X-ray scattering

Cosma D. Dellisanti<sup>a,1</sup>, Silvia Spinelli<sup>b</sup>, Christian Cambillau<sup>b</sup>, John B.C. Findlay<sup>a</sup>, Peter F. Zagalsky<sup>c</sup>, Stéphanie Finet<sup>d</sup>, Véronique Receveur-Bréchet<sup>b,\*</sup>

<sup>a</sup>School of Biochemistry and Molecular Biology, University of Leeds, Mount Preston Street, Leeds LS2 9JT, UK

<sup>b</sup>Architecture et Fonction des Macromolécules Biologiques, UMR 6098 CNRS, 31 Chemin Joseph Aiguier, 13402 Marseille Cedex 20, France

<sup>c</sup>School of Biological Sciences, Royal Holloway College, University of London, Egham Hill, Egham TW20 0EX, UK

<sup>d</sup>European Synchrotron Radiation Facility, BP 220, 38043 Grenoble Cedex, France

Received 10 January 2003; revised 7 April 2003; accepted 28 April 2003

First published online 14 May 2003

Edited by Irmgard Sinning

**Abstract** The structure of  $\alpha$ -crustacyanin, the blue carotenoprotein of lobster (*Homarus gammarus*) carapace, has been investigated for the first time using small-angle X-ray scattering. In this paper, we have determined the dimensions of this protein composed of eight heterodimeric subunits of  $\beta$ -crustacyanin. Analysis of the scattering spectra and estimation of the shape of  $\alpha$ -crustacyanin show that the protein fits into a cylinder with an axial length of 238 Å and a radius of 47.5 Å, in which the eight  $\beta$ -crustacyanin molecules are probably arranged in a helical manner.

© 2003 Federation of European Biochemical Societies. Published by Elsevier Science B.V. All rights reserved.

**Key words:** Small-angle X-ray scattering; Carotenoprotein; Lipocalin; Quaternary structure

## 1. Introduction

The lipocalin family gathers together numerous secreted small proteins (typically ~20 kDa) with great functional diversity that share several common molecular-recognition properties. Among them are examples with remarkable ability to bind small, usually hydrophobic, molecules with critical biological function such as retinoids, odorants, etc. [1]. Characterising their biological and structural properties is of major interest and importance in understanding their particular specificity in molecular recognition in the various mechanisms of critical biological processes such as vision, pigmentation, olfaction, etc.

A number of lipocalins are involved in invertebrate colouration. Thus, the typical blue colouration of lobster (*Homarus gammarus*) carapace is due to the carotenoprotein  $\alpha$ -crustacyanin. This protein is a hexadecamer organised as an octamer of heterodimers, the  $\beta$ -crustacyanins. Five electrophoretically distinct monomers have been identified, grouped into two types: A<sub>2</sub> and A<sub>3</sub> (CRTA type); C<sub>1</sub>, C<sub>2</sub> and A<sub>1</sub> (CRTC type) [2]. Among the possible combinations of monomers to

form  $\beta$ -crustacyanin, by far the most abundant is one A<sub>2</sub> and one C<sub>1</sub> subunit [3]. The crystal structures of two monomeric CRTC subunits, i.e. A<sub>1</sub> and C<sub>1</sub>, have recently been solved by crystallographic methods [4,5], revealing a  $\beta$ -barrel made of eight anti-parallel  $\beta$ -strands arranged in two orthogonal  $\beta$ -sheets continuously hydrogen-bonded, typical of the lipocalin fold.

Each apocrustacyanin subunit can bind a single molecule of the carotenoid astaxanthin (3,3'-dihydroxy- $\beta$ , $\beta$ -carotene-4,4'-dione). The protein-bound astaxanthin in crustacyanin is able to undergo large bathochromic shifts in light absorption spectrum from 472 nm for free astaxanthin to 580–590 nm for  $\beta$ -crustacyanin, and to 632 nm for  $\alpha$ -crustacyanin [6]. One of the main interests in  $\alpha$ -crustacyanin originally lay in the similarity of the spectral shift of astaxanthin in crustacyanin to that of retinal in the rod visual pigment rhodopsin. Since then, many studies have tried to address the question of this bathochromic shift [7–13]. The spectral shift depends on heterodimer formation, and additionally the presence of astaxanthin is essential for the dimer stability. Very recently, Cianci and co-workers [14] have succeeded in solving the crystal structure of the A<sub>1</sub>–A<sub>3</sub>  $\beta$ -crustacyanin, shedding light on the molecular basis of this process. They have shown that the two bound carotenoids interpenetrate the A<sub>1</sub> to A<sub>3</sub> interface, with each subunit containing half of each carotenoid in a hydrophobic cavity. The bathochromic shift would arise from a coplanarisation of the end rings with the polyene chain and from a polarisation of the ligand thanks to hydrogen bonding through two bound water molecules resulting in a permanent induced dipole moment of astaxanthin.

However, the further spectral shift to 632 nm observed in  $\alpha$ -crustacyanin remains unexplained. The  $\beta$ -crustacyanins are irreversible dissociation products of  $\alpha$ -crustacyanin, which suggests that strong and specific interactions between the subunits and with the carotenoid responsible for the cohesion of the quaternary structure of  $\alpha$ -crustacyanin may be critical for this bathochromic shift. While crystals of  $\alpha$ -crustacyanin have been obtained [15], no structure ever emerged from it so far, therefore its atomic structure is still unknown. An old study on the quaternary structure of  $\alpha$ -crustacyanin using electron microscopy was reported in [16]. Unfortunately, the rather poor quality of the electron micrographs leads to ambiguities in their interpretation. The authors nevertheless proposed two putative models of the scaffolding of  $\alpha$ -crustacyanin. In the first model eight  $\beta$ -crustacyanins are assembled as a compact

\*Corresponding author. Fax: (33)-4 91 16 45 36.

E-mail address: [receveur@afmb.cnrs-mrs.fr](mailto:receveur@afmb.cnrs-mrs.fr) (V. Receveur-Bréchet).

<sup>1</sup> Present address: Laboratori di Biologia Strutturale, Sincrotrone Elettra, S.S. 14–km 163.5, 34012 Basovizza (TS), Italy.

double tetramer, with the two tetramers facing each other with the subunits of one positioned in the grooves between the subunits of the other. In the second, the  $\beta$ -crustacyanins are arranged in a linear array, forming a helical coil with four to five dimers per turn. Since this report, no further study of this nature has been reported. Therefore, in order to obtain a more precise description of its quaternary structure, we have carried out small-angle X-ray scattering experiments on  $\alpha$ -crustacyanin. Small-angle X-ray scattering is a powerful technique to determine the scaffolding of macromolecular complexes whose subunit structures are known [17–19]. In the present study, we have established the dimensions of the  $\alpha$ -crustacyanin assembly and inferred the first information on the global shape of the protein.

## 2. Materials and methods

### 2.1. Experimental procedure

Native  $\alpha$ -crustacyanin was extracted from the lobster (*Homarus gammarus*) carapace and purified as described in [6]. The protein was then extensively dialysed in 10 mM Tris pH 7.0, 50 mM NaCl, with addition of 10% v/v glycerol as radiation scavenger. In this buffer, the absorption spectrum of the protein in the 560–650 nm region exhibits no peak corresponding to  $\beta$ -,  $\alpha'$ - or  $\gamma$ -crustacyanin, and its profile is exactly the same as in this buffer without glycerol. This means that  $\alpha$ -crustacyanin is indeed the only structural form present in solution and is not altered by the presence of glycerol in solution. The protein was finally concentrated to 30.8 mg/ml with Centricon 50 (Amicon) concentrator tubes in a Multifuge 3S-R Heræus (Sorvall) centrifuge.

Data collection was recorded at the European Synchrotron Radiation Facility (ESRF, Grenoble, France), on beamline ID02. The wavelength was set at 1.0 Å. The sample-to-detector distances were set at 3.0 and 1.0 m, leading to scattering vectors  $q$  ranging from 0.008 to 0.22 Å<sup>-1</sup> and from 0.030 to 0.5 Å<sup>-1</sup>, respectively. The scattering vector is defined as  $q = (4\pi/\lambda)\sin\theta$ , where  $2\theta$  is the scattering angle. The detector was a Thomson X-ray image intensifier optically coupled to an ESRF developed FReLoN CCD camera. Collections made of 30 successive frames of 0.5 s with 4 s intervals (dead time) between each frame were recorded for each sample. During the dead-time, fresh protein solution was pushed into a 1.5 mm Lindemann-type quartz capillary by using a remote-controlled syringe coupled with the data acquisition programme, so that no protein solution was irradiated longer than half a second. Background scattering was measured after each protein sample using the buffer solution.

The protein concentration was varied from 1.8 to 13 mg/ml in order to check for interparticle interactions and all dilutions were prepared in the dialysis buffer from the 30.8 mg/ml protein stock solution. The temperature was set at 20°C. The protein concentrations were measured by absorbance at 280 nm using the extinction coefficient  $\epsilon = 1.38$  ml mg<sup>-1</sup> cm calculated from the sequence [20].

### 2.2. Data treatment

Each protein or buffer frame was carefully inspected to check for possible bubble formation or radiation-induced aggregation effects on the scattering pattern. No radiation-induced damage was observed, allowing individual frames to be averaged. Averaged data sets of buffer from the immediately following collection were subtracted from the protein scattering patterns after proper normalisation and correction from detector response. Absolute calibration was made with a Lupolen sample, a polymer thoroughly characterised and used as a standard on the ID02 beamline for the conversion of the measured scattering patterns of any sample into absolute intensities [21]. The data acquired at both sample-to-detector distances of 3 and 1 m were merged for the calculations using the entire scattering spectrum.

### 2.3. Scattering data analysis

The value of the radius of gyration  $R_g$  can be derived from the scattering spectra using the Guinier approximation  $I(q) = I(0) \times \exp(-q^2 R_g^2/3)$  [22], where  $I(q)$  is the scattered intensity and  $I(0)$  is the forward scattering intensity. In dilute solution,  $I(0)/c$  is proportional to the molecular mass  $M$  of the scattering object, where  $c$  is its

concentration, and to the excess scattering of the object relative to the buffer according to the following equation [23]:

$$I(0) = \frac{cM}{N} [(\rho_p - \rho_s)\bar{v}_p]^2$$

$N$  is Avogadro's constant,  $\rho_p$  is the scattering length density of the protein,  $\rho_s$  the scattering length density of the buffer taking into account the presence of 10% v/v glycerol and  $\bar{v}_p$  is the partial specific volume of the protein.

In the case of rod-shaped particles, the scattering intensity  $I(q)$  is related to the scattering vector  $q$  by the equation [24]:

$$\text{Ln}(qI(q)) = \text{Ln}(I_c(0)) - \frac{q^2 R_c^2}{2}$$

where  $I_c(q) = qI(q)$  and  $R_c$  is the radius of cross-section. This equation is only valid for  $2\pi/L < q < 1/R_c$ , where  $L$  is the length of the rod-like particle defined by  $L = \pi I(0)/I_c(0)$  [24].

The distance distribution function  $P(r)$  was calculated by the Fourier inversion of the scattering intensity  $I(q)$  using both programmes GNOM [25] and GIFT [26].

## 3. Results

### 3.1. Determination of the radius of gyration

The radii of gyration of  $\alpha$ -crustacyanin at six different concentrations have been inferred from the slope and the intercept of the linear fit of  $\text{Ln}[I(q)]$  vs  $q^2$  for  $q \times R_g \leq 1.3$ . The plots in Fig. 1 show that  $\alpha$ -crustacyanin follows very well the Guinier law for every protein concentration. The  $R_g$  extrapolated at zero concentration has been found to be  $76.1 \pm 0.6$  Å, and some slight repulsive intermolecular interactions in the solution were observed as the radius of gyration increased when the concentration decreased. The  $I(0)/c$  value of 18.2 obtained experimentally corresponds to a molecular weight of 305 kDa, according to the amino acid composition of  $\alpha$ -crustacyanin and to the excess scattering of  $\alpha$ -crustacyanin in the buffer used here. This is in excellent agreement with the expected molecular weight of ca 320 kDa and confirms that  $\alpha$ -crustacyanin is present in solution as a hexadecameric complex.

### 3.2. Distance distribution function

The distance distribution function  $P(r)$  is the histogram of all the interatomic distances within a molecule. This function provides the maximum dimension  $D_{\text{max}}$  of the molecule, which is defined as the point where  $P(r)$  becomes zero. Fig.

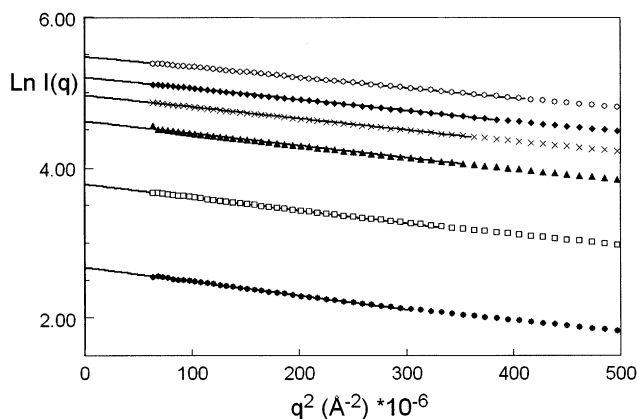


Fig. 1. Guinier plot of the scattering profiles of  $\alpha$ -crustacyanin. The protein concentrations are: full circles, 1.8 mg/ml; empty squares, 3.1 mg/ml; full triangles, 6.0 mg/ml; crosses, 7.8 mg/ml; full diamonds, 9.1 mg/ml; empty circles, 13.0 mg/ml.

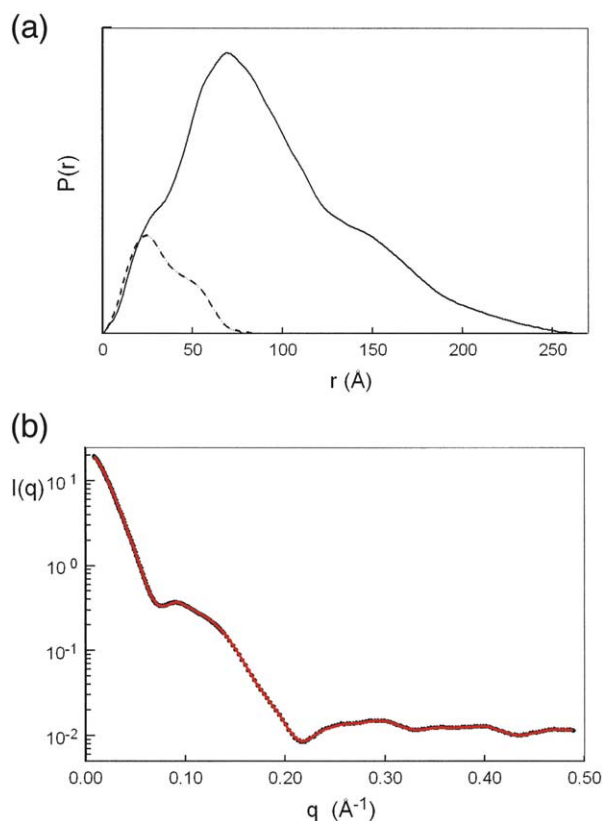


Fig. 2. a: Distance distribution function  $P(r)$  of  $\alpha$ -crustacyanin (continuous line) and of  $\beta$ -crustacyanin (dashed line). b: Corresponding fit (red line) on the experimental scattering curve of  $\alpha$ -crustacyanin.

2 shows the  $P(r)$  function obtained experimentally for  $\alpha$ -crustacyanin, superimposed by the  $P(r)$  function calculated from the 3D coordinates of  $\beta$ -crustacyanin (pdb code 1GKA) using CRY SOL [27] and GNOM. The maximum distance obtained for  $\alpha$ -crustacyanin ( $D_{\max} = 263 \pm 3$  Å) and the shape of the  $P(r)$  function indicate that the protein has an elongated shape. The left shoulder of the main peak matches with the maximum of the  $P(r)$  function of  $\beta$ -crustacyanin ( $r_1 = 25$  Å). The

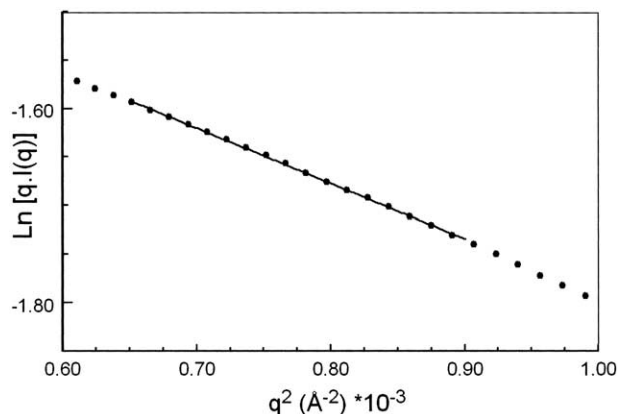


Fig. 3.  $\text{Ln}[qI(q)]$  vs  $q^2$  plot in the medium- $q$  region and linear regression curve for  $\alpha$ -crustacyanin.

major peak ( $r_2 = 67$  Å) corresponds to the most frequent distance within  $\alpha$ -crustacyanin. It may indicate distances between the most repetitive motifs in this octameric complex of  $\beta$ -crustacyanin. Finally, the broad right shoulder of this peak ( $r_3 = 130$ – $140$  Å) may correspond to a second-order repetition of the same motif ( $r_3 \approx 2 r_2$ ).

The  $P(r)$  function enables an alternative calculation of  $R_g$  using the entire scattering curve ( $R_g$  is estimated from the second moment of the  $P(r)$  function). The  $R_g$  value obtained through this method is  $73.3 \pm 0.1$  Å, which is consistent with the value calculated by the Guinier approximation.

### 3.3. Rod-like particle model

As the distance distribution function of  $\alpha$ -crustacyanin indicates that it is elongated, we have analysed the scattering intensities by assuming that it could have the shape of a rod. If so, the plot  $\text{Ln}[qI(q)]$  vs  $q^2$  should be linear in the medium-angle region. The results shown in Fig. 3 indeed suggest that  $\alpha$ -crustacyanin has the shape of a rod. The radius of cross-section  $R_c$  and the length of the particle  $L$  have been inferred, respectively, from the slope and the intercept of the linear fit of the plot  $\text{Ln}[qI(q)]$  vs  $q^2$  in the appropriate  $q$  region. This

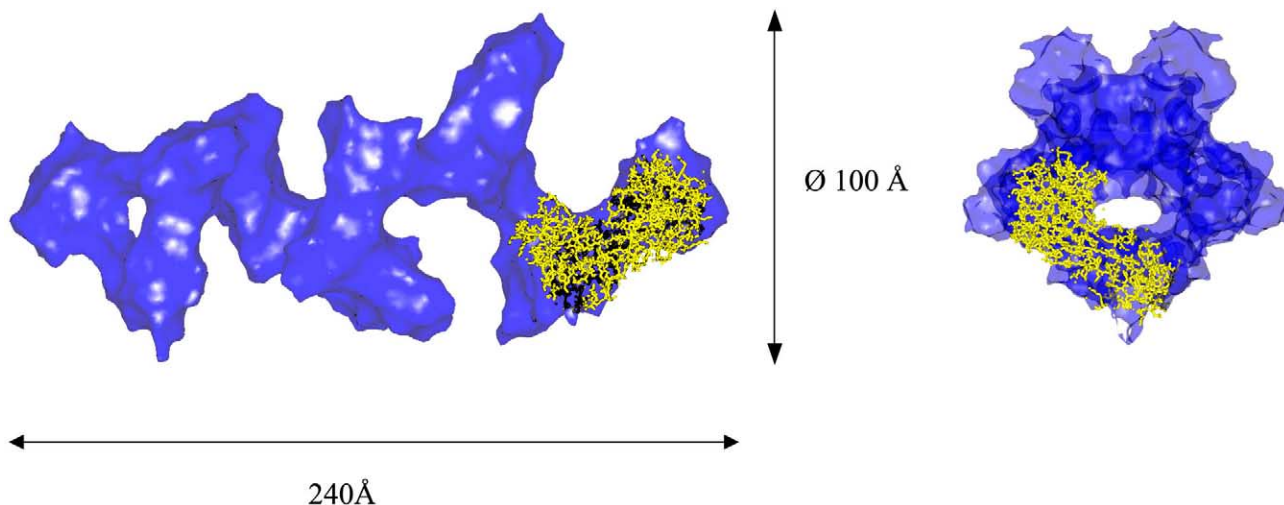


Fig. 4. Example of the helical shape of  $\alpha$ -crustacyanin obtained with the programme GASBOR. The crystal structure of one heterodimeric subunit (yellow) has been inserted in the shape. The figure has been obtained with Accelrys ViewerPro<sup>®</sup>.

leads to values of  $33.6 \pm 0.3 \text{ \AA}$  for  $R_c$  and  $238 \pm 1 \text{ \AA}$  for  $L$ . If the rod has a circular cross-section, the radius  $R$  is related to  $R_c$  by the equation:  $R = \sqrt{2}R_c$ , that is  $47.5 \text{ \AA}$  for  $\alpha$ -crustacyanin. The radius of gyration of a cylinder is given by  $R_g^2 = L^2/12 + R^2/2$  [24,28], which leads to  $76.4 \text{ \AA}$  in our case. This is in excellent agreement with the value obtained by the Guinier approximation. Moreover, we can calculate the maximum distance in a cylinder of length  $238 \text{ \AA}$  and of radius  $47.5 \text{ \AA}$ , resulting in a  $D_{\max}$  of  $256 \text{ \AA}$ . This is also absolutely consistent with the value obtained independently from the  $P(r)$  function. It is noteworthy that the model of a rod-like particle can be applied only if  $D_{\max}/2R > 2.5$ , which is the case here.

#### 4. Discussion

In the work presented here, small-angle X-ray scattering experiments carried out on  $\alpha$ -crustacyanin have allowed the first description of the geometry of this hexadecameric complex, showing that it can fit into a cylinder of  $238 \text{ \AA}$  length, with a diameter of  $95 \text{ \AA}$ . Using different ab initio programmes such as DAMMIN [29], GASBOR [30] DALAI\_GA [31] and SAXS3D [32], we have tried to restore the shape of  $\alpha$ -crustacyanin. Unfortunately, our calculations did not converge to a unique solution. Due to the intrinsic degeneracy of the inverse scattering problem these programmes can inevitably lead to incorrect structures which nevertheless are able to fit the scattering curve. To limit this, it is necessary to repeat such calculations a sufficient number of times in order to find a reproducible solution. In our case, we have run every programme at least several dozen of times, with or without any symmetry restrictions, with different size of beads, on the entire curve or on the truncated curve where the large-angle region was removed. Unfortunately, we were unable to obtain a really reproducible shape. Some common features are, however, recurrent. The shapes are always cylindrical, with a length of  $220$ – $250 \text{ \AA}$  and a diameter of  $90$ – $100 \text{ \AA}$ , confirming our previous analysis. Moreover, the cylinder is never fully filled but contains many large crevices. Indeed, the volume of the scattering particle can be determined by:  $V = 2\pi^2 I(0)/Q$  where the invariant  $Q$  is given by  $Q = \int_0^\infty I(q)q^2 dq$  [33]. The scattering spectrum of  $\alpha$ -crustacyanin leads to a value of  $6 \times 10^5 \text{ \AA}^3$ , which corresponds exactly to the external volume eight  $\beta$ -crustacyanins according to their crystal structure. The volume of a cylinder of  $238 \text{ \AA}$  length and of diameter  $95 \text{ \AA}$  is, however, equal to  $17 \times 10^5 \text{ \AA}^3$ , confirming the existence of large holes within it. As the crevices are positioned differently from one calculated envelope to another, averaging of these envelopes using SUPCOMB [34] leads to a filled cylinder. However, the pattern of these crevices always suggests a more or less helical shape of the protein. Fig. 4 shows an example of the envelope obtained using GASBOR ( $\chi^2 = 6.7$ ), with an inset of one  $\beta$ -crustacyanin, clearly representing a helical scaffolding. Even if this shape does not represent the real organisation of  $\alpha$ -crustacyanin, it at least provides an overview of the putative structural organisation that the protein may adopt. The complexity of this non-globular scaffolding containing many discontinuities as well as the relatively large size of the protein (2840 residues) may be the reasons why the limits of the classical ab initio shape-restoration programmes have, unfortunately, in this case been exceeded. The lack of any precise envelope has also prevented us from finding a model of a scaffold made of eight copies of the crystal

structure of  $\beta$ -crustacyanin that would have fit the data using CRY SOL [27].

Finally, our results go in the same direction as the initial model of Zagalsky and Jones [16] that proposed a helical arrangement of the eight  $\beta$ -crustacyanins in  $\alpha$ -crustacyanin. The dimensions of their proposed scaffold ( $85 \text{ \AA} \times 135 \text{ \AA}$  for  $\alpha$ -crustacyanin and spheres of  $51 \text{ \AA}$  for  $\beta$ -crustacyanin instead of ca  $44 \text{ \AA} \times 75 \text{ \AA}$  according to the crystal structure) does not correspond to those derived here, but this could be due to a probable arrangement of the proteins perpendicularly to the grid during staining. Therefore, in order to refine our model and to elucidate the exact way the eight  $\beta$ -crustacyanins are disposed with respect to each other in  $\alpha$ -crustacyanin, cryo-electron microscopy studies coupled with comparison of the experimental scattering pattern and 3D modelling based on the crystal structure of the individual subunits are being undertaken.

*Acknowledgements:* C.D.D. was supported by Grant No. B104-CT98-0420 from the European Community.

#### References

- [1] Flower, D.R. (1996) *Biochem. J.* 318, 1–14.
- [2] Quarmby, R., Norden, D.A., Zagalsky, P.F., Ceccaldi, H.J. and Daumas, R. (1977) *Comp. Biochem. Physiol.* 56, 55–61.
- [3] Keen, J.N., Caceres, I., Eliopoulos, E.E., Zagalsky, P.F. and Findlay, J.B.C. (1991) *Eur. J. Biochem.* 197, 407–417.
- [4] Cianci, M., Rizkallah, P.J., Olczak, A., Raftery, J., Chayen, N.E., Zagalsky, P.F. and Helliwell, J.R. (2001) *Acta Cryst.* D57, 1219–1229.
- [5] Gordon, E.J., Leonard, G.A., McSweeney, S. and Zagalsky, P.F. (2001) *Acta Cryst.* D57, 1230–1237.
- [6] Zagalsky, P.F. (1985) *Methods Enzymol.* 111, 216–247.
- [7] Salares, V.R., Young, N.M., Carey, P.R. and Bernstein, H.J. (1977) *J. Raman Spectrosc.* 6, 282–288.
- [8] Salares, V.R., Young, N.M., Bernstein, H.J. and Carey, P.R. (1979) *Biochim. Biophys. Acta* 576, 176–191.
- [9] Keen, J.N., Caceres, I., Eliopoulos, E.E., Zagalsky, P.F. and Findlay, J.B.C. (1991) *Eur. J. Biochem.* 202, 31–40.
- [10] Weesie, R.J., Askin, D., Jansen, F.J.H.M., de Groot, H.J.M., Lugtenburg, J. and Britton, G. (1995) *FEBS Lett.* 362, 34–38.
- [11] Weesie, R.J., Jansen, F.J.H.M., Merlin, J.C., Lugtenburg, J., Britton, G. and de Groot, H.J.M. (1997) *Biochemistry* 36, 7288–7296.
- [12] Britton, G., Weesie, R.J., Askin, D., Warburton, J.D., Gallardo-Guerrero, L., Jansen, F.J.H.M., de Groot, H.J.M., Lugtenburg, J., Cornard, J.P. and Merlin, J.C. (1997) *Pure Appl. Chem.* 69, 2075–2084.
- [13] Weesie, R.J., Verel, R., Jansen, F.J.H.M., Britton, G., Lugtenburg, J. and de Groot, H.J.M. (1997) *Pure Appl. Chem.* 69, 2085–2090.
- [14] Cianci, M., Rizkallah, P.J., Olczak, A., Raftery, J., Chayen, N.E., Zagalsky, P.F. and Helliwell, J.R. (2002) *Prot. Natl. Acad. Sci. USA* 99, 9795–9800.
- [15] Cheesmad, D.F., Zagalsky, P.F. and Ceccaldi, H.J. (1966) *Proc. R. Soc. B* 164, 130–151.
- [16] Zagalsky, P.F. and Jones, R. (1982) *Comp. Biochem. Physiol.* 71, 237–242.
- [17] Fetler, L. and Vachette, P. (2001) *J. Mol. Biol.* 309, 817–832.
- [18] Macol, C.P., Tsuruta, H., Stec, B. and Kantrowitz, E.R. (2001) *Nat. Struct. Biol.* 8, 423–426.
- [19] Receveur, V., Czjzek, M., Schulein, M., Panine, P. and Henrissat, B. (2002) *J. Biol. Chem.* 277, 40887–40892.
- [20] Zagalsky, P.F. (1994) *Pure Appl. Chem.* 66, 973–980.
- [21] Bosecke, P. and Diat, O. (1997) *J. Appl. Cryst.* 30, 867–871.
- [22] Guinier, A. and Fournet, G. (1955) *Small Angle Scattering of X-Rays*, Wiley Interscience, New York.
- [23] Zacc a, G. and Jacrot, B. (1983) *Ann. Rev. Biophys. Bioeng.* 12, 139–157.
- [24] Feigin, L.A. and Svergun, D.I. (1987) *Structure Analysis by*

- Small-Angle X-Ray and Neutron Scattering, Plenum Press, New York.
- [25] Svergun, D.I. (1992) *J. Appl. Cryst.* 25, 495–503.
- [26] Bergmann, A., Fritz, G. and Glatter, O. (2000) *J. Appl. Cryst.* 33, 1212–1216.
- [27] Svergun, D.I., Barberato, C. and Koch, M.H.J. (1995) *J. Appl. Cryst.* 28, 768–773.
- [28] Porod, G. (1982) in: *Small Angle X-Ray Scattering* (Glatter, O. and Kratky, O., Eds.), pp. 17–53, Academic Press, New York.
- [29] Svergun, D.I. (1999) *Biophys. J.* 76, 2879–2886.
- [30] Svergun, D.I., Petoukhov, M.V. and Koch, M.H. (2001) *Biophys. J.* 80, 2946–2953.
- [31] Chacón, P., Morán, F., Díaz, J.F., Pantos, E. and Andreu, J.M. (1998) *Biophys. J.* 74, 2760–2775.
- [32] Walther, D., Cohen, F.E. and Doniach, S. (2000) *J. Appl. Cryst.* 33, 350–363.
- [33] Glatter, O. (1982) in: *Small Angle X-Ray Scattering* (Glatter, O. and Kratky, O., Eds.), pp. 119–167, Academic Press, New York.
- [34] Kozin, M.B. and Svergun, D.I. (2000) *J. Appl. Cryst.* 34, 33–41.